

Generation and transport of Reactive Nitrogen species in Surface Barrier Discharges

Aaron Dickenson, Nikolay Britun, Anton Nikiforov, Christophe Leys, Mohammad Hasan, and James Walsh

Supplementary material: Details of numerical model

The numerical model used in this study consisted of a reactive flow model couple with a plasma physics module and chemistry module. This approach was adopted to enable modelling of physicochemical phenomena extending over 6 orders of magnitude in time and 4 orders of magnitude in space with reasonable computational run times. Each of the two modules and the main model (alternatively the three modules) were defined over a range of scales in space and time. A summary of the modules and the corresponding scales in space and time is given in table 1.

Module	Spatial dimensions	Spatial scale	Temporal scale
Plasma module	2D	μm to mm	ns to μs
Chemistry module	0D (global model)	--	tens of μs to ms
Reactive flow module	2D	mm to cm	Tens of ms to s

Table 1. A summary of the three modules and the scales over which they are defined.

1. Plasma module

The plasma module was a 2D time dependent multi-fluid model. Its inputs were the applied waveform and the discharge geometry. The computational domain of the plasma module is shown in figure 1. Considering the short timescales covered by the plasma module, the gas temperature was assumed to be equal to the room temperature and the convective flow was ignored. The plasma module was solved for one period of the applied waveform.

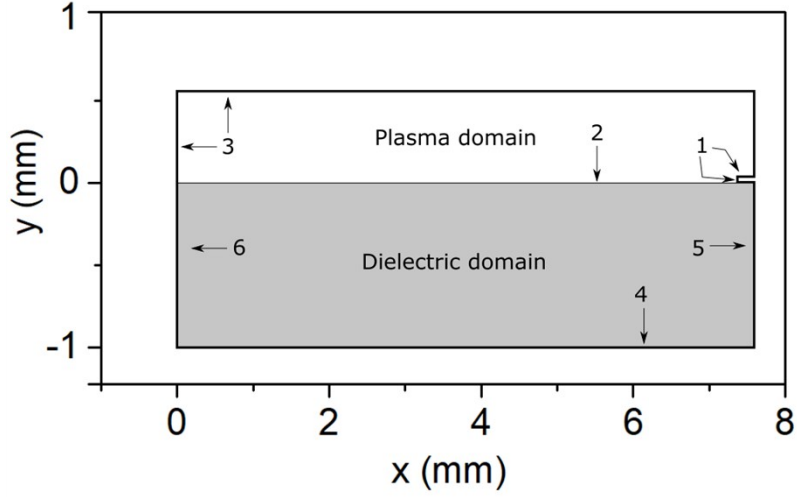


Figure 1. The computational domain of the plasma module. The electrode is enlarged for clarity. The numbers shown indicate the boundary conditions defined in table 3.

The variables solved for in the module were the electric potential V (V), the electron density n_e (m^{-3}), the electron energy density n_{en} ($\text{eV}\cdot\text{m}^{-3}$), the surface charge density on the dielectric surface ρ_s ($\text{C}\cdot\text{m}^{-2}$), and the densities of N_2^+ , O_2^+ , and O_2^- , represented by the variables $n_{N_2^+}$ (m^{-3}), $n_{O_2^+}$ (m^{-3}), and $n_{O_2^-}$ (m^{-3}), in addition to the background gas species, N_2 and O_2 , which constitute 79% and 21% of air respectively. To calculate the electric potential, the Poisson equation (equation 1) was solved in the plasma domain and in the dielectric domain, emphasised in figure 1 [1].

$$\nabla^2 V = \frac{-e}{\varepsilon} (n_{N_2^+} + n_{O_2^+} - n_{O_2^-} - n_e) \quad (1)$$

In equation 1, e is the electron charge (C) and ε is the dielectric permittivity ($\text{F}\cdot\text{m}^{-1}$), which is assumed to be 4.7 in the dielectric material and 1 in air. To calculate the densities of all species, the continuity equation, in drift-diffusion form as given by equation 2, was solved for every species in the plasma region only [1].

$$\frac{\partial n_i}{\partial t} + \nabla \cdot (-n_i \mu_i \nabla V - D_i \nabla n_i) = R_i \quad (2)$$

In equation 2, n_i is the density of the i^{th} species, μ_i is the mobility of the i^{th} species ($\text{m}^2 \cdot \text{V}^{-1} \cdot \text{s}^{-1}$), D_i is the diffusion coefficient of the i^{th} species ($\text{m}^2 \cdot \text{s}^{-1}$). For ions and neutral species, the diffusion coefficients were obtained from [2], and the mobilities for the ionic species were calculated using Einstein's relation [3]. For electrons, the mobility and the diffusion coefficient were calculated using BOLSIG+ and tabulated as functions of the mean electron energy [4,5]. The last term R_i is the rate expression of the i^{th} species where all generation and loss terms are included in that term. A typical expansion of the term R_i is given in equation 3.

$$R_i = k_a n_A n_B - k_b n_i n_C + \dots \quad (3)$$

In equation 3, k_a and k_b are the rate coefficients of reactions a and b respectively ($\text{m}^3 \cdot \text{s}^{-1}$), species A and B are the reactants of reaction a while species i and C are reactants for reaction b . The first term is positive indicating that reaction a is a generation reaction for the i^{th} species, while the second term is negative indicating that reaction b is a loss reaction of the species i . Equation 3 has a term for every reaction where the i^{th} species is either a product or a reactant. A list of the reactions included in the plasma module is given in table 2.

The surface charge density ρ_s ($\text{C} \cdot \text{m}^{-2}$) in the plasma module was defined on the dielectric surface and is governed by equation 4 [6].

$$\frac{\partial \rho_s}{\partial t} = e \hat{n} \cdot \left(\vec{\Gamma}_{N_2^+} + \vec{\Gamma}_{O_2^+} - \vec{\Gamma}_{O_2^-} - \vec{\Gamma}_e \right) \quad (4)$$

In equation 4, \hat{n} is the normal unit vector on the dielectric surface, and $\vec{\Gamma}_i$ is the flux of the i^{th} species on the surface ($\text{m}^{-2} \cdot \text{s}^{-1}$). The electron energy density equation is governed by equation 5.

$$\frac{\partial n_{en}}{\partial t} + \nabla \cdot \left(-\mu_{en} n_{en} \nabla V - D_{en} \nabla n_{en} \right) = S_{en} - \nabla V \cdot \vec{\Gamma}_e \quad (5)$$

In equation 5, μ_{en} ($\text{m}^2 \cdot \text{V}^{-1} \cdot \text{s}^{-1}$) and D_{en} ($\text{m}^2 \cdot \text{s}^{-1}$) are the electron energy mobility and diffusion coefficient respectively, both were calculated using BOLSIG+ [4,5]. The term S_{en} represents the collisional energy loss by the electrons. Essentially, it is similar to the expression given in equation 3 but with the energy cost of every reaction multiplied by the rate coefficient of the corresponding reaction. The last term in equation 5 is the ohmic heating term, where $\vec{\Gamma}_e$ is the electron flux.

Rxn No	Reaction formula	Reaction coefficient	Energy cost (eV)	Ref.
R1	$e + \text{N}_2 \rightarrow e + \text{N}_2$	$f(\mathcal{E}_{avg})$	$0.3(T_e - T_g)$	[2]
R2	$e + \text{O}_2 \rightarrow e + \text{O}_2$	$f(\mathcal{E}_{avg})$	$0.26(T_e - T_g)$	[2]
R3	$e + \text{N}_2 \rightarrow 2e + \text{N}_2^+$	$1 \times 10^{-16} \mathcal{E}_{avg}^{1.9} \exp(-14.6/\mathcal{E}_{avg})$	15.58	[2]
R4	$e + \text{O}_2 \rightarrow 2e + \text{O}_2^+$	$9.54 \times 10^{-12} \mathcal{E}_{avg}^{-1.05} \exp(-55.6/\mathcal{E}_{avg})$	12.07	[2]
R5	$e + \text{O}_2 \rightarrow \text{O}_2^-$	$9.72 \times 10^{-15} \mathcal{E}_{avg}^{-1.62} \exp(-14.2/\mathcal{E}_{avg}) \mathcal{E}_{avg} > 1.13$ $2.78 \times 10^{-20} \mathcal{E}_{avg} < 1.13$		[2]
R6	$e + \text{N}_2 + \text{O}_2 \rightarrow \text{N}_2 + \text{O}_2^-$	$1.1 \times 10^{-43} (T_g/T_e)^2 \exp(-70/T_g) \exp(1500(T_e - T_g)/(T_e T_g))$		[2]
R7	$e + 2\text{O}_2 \rightarrow \text{O}_2 + \text{O}_2^-$	$1.4 \times 10^{-41} (T_g/T_e) \exp(-600/T_g) \exp(700(T_e - T_g)/(T_e T_g))$		[2]
R8	$M + e + \text{N}_2^+ \rightarrow M + \text{N}_2$	$3.12 \times 10^{-35}/T_e$		[2]
R9	$\text{N}_2 + \text{O}_2^- \rightarrow e + \text{O}_2 + \text{N}_2$	$1.9 \times 10^{-18} (T_g/300)^{0.5} \exp(-4990/T_g)$		[2]
R10	$\text{O}_2 + \text{O}_2^- \rightarrow e + \text{O}_2 + \text{O}_2$	$2.7 \times 10^{-16} (T_g/300)^{0.5} \exp(-5590/T_g)$		[2]
R11	$\text{O}_2 + \text{N}_2^+ \rightarrow \text{O}_2^+ + \text{N}_2$	5×10^{-17}		[2]
R12	$\text{O}_2^- + \text{N}_2^+ \rightarrow \text{O}_2 + \text{N}_2$	$2 \times 10^{-13} (300/T_g)^{0.5}$		[2]
R13	$\text{O}_2^- + \text{O}_2^+ \rightarrow 2\text{O}_2$	$2 \times 10^{-13} (300/T_g)^{0.5}$		[2]

Table 2. A list of reactions included in the plasma module.

In table 2, \mathcal{E}_{avg} is the mean electron energy (eV), calculated from n_{en}/n_e [4], T_g is the gas temperature (K), and T_e is the electron temperature (eV), defined as $2\mathcal{E}_{avg}/3$. The rate coefficients of reactions 1 and 2 were calculated using BOLSIG+ [4], with the cross sections used obtained from [5].

For every equation solved in the plasma module, a boundary condition was defined over every edge in the computational domain. The boundary conditions are listed in table 3, where the number of the boundary is indicated in figure 1.

Boundary	Electric potential	Continuity equations
1	$V = V_{applied}$	$\hat{n} \cdot \vec{\Gamma}_i = \frac{1}{4} n_i v_{th,i} - \mu_i n_i \nabla V (-\nabla V \cdot \hat{n} > 0)$
2	$-\epsilon \nabla V = \rho_s$	$\hat{n} \cdot \vec{\Gamma}_i = \frac{1}{4} n_i v_{th,i} - \mu_i n_i \nabla V (-\nabla V \cdot \hat{n} > 0)$
3	$-\hat{n} \cdot \nabla V = 0$	$\hat{n} \cdot \vec{\Gamma}_i = 0$
4	$V = 0$	N/A
5	$-\hat{n} \cdot \nabla V = 0$	N/A
6	$-\hat{n} \cdot \nabla V = 0$	N/A

Table 3. A list of boundary conditions used in the plasma module.

In table 3, $V_{applied}$ is the applied voltage waveform obtained from experiments, $v_{th,i}$ is the thermal speed of the i^{th} species. The condition in parenthesis for continuity equation on boundary 1 and 2 is non-zero only if the flux driven by the electric field is directed outward of the computational domain. Boundary 1 represented the driven electrode, boundary 2 represented the interface between the plasma and the dielectric, where the flux of the charged species created a surface charge, boundary 3 represented a symmetry boundary implying that the outer side of the boundary is a mirrored version of the domain, and boundary 4 was the ground.

As the plasma module was solved, the instantaneous Electrohydrodynamic force (given in equation 6) and the electron energy density were integrated in time [6]. When the module had finished running the integrated variables were divided by the period of the waveform, giving the time-averaged variables.

$$F_{inst} = -e \left(n_{N_2^+} + n_{O_2^+} - n_{O_2^-} - n_e \right) \nabla V \quad (6)$$

The time-averaged electron energy density was normalised and defined as the extrapolation parameter S . The importance of this parameter is that it indicated the regions in the computational domain where electron impact reactions have the highest intensity.

2. Chemistry module:

The extrapolation parameter S , obtained from the plasma module, is shown in figure 2. It clearly shows that the electron driven chemistry occurs mainly at a point close to the driven electrode. For this reason, it was assumed that this point is the domain of the chemistry module.

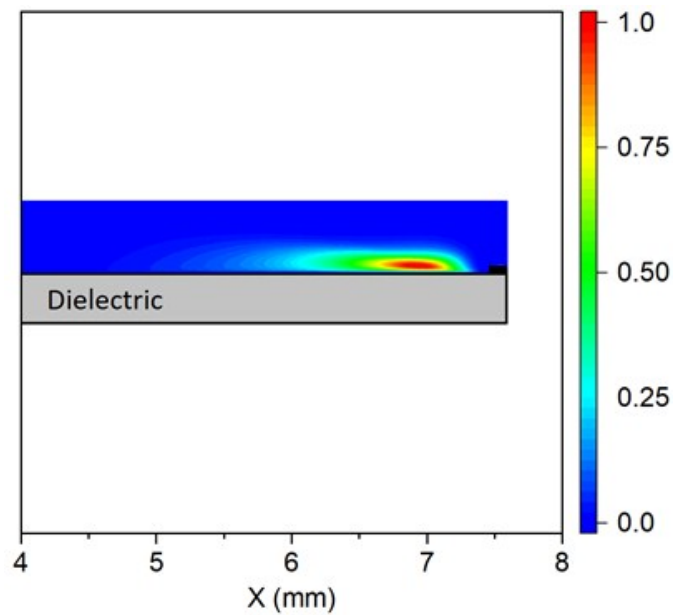


Figure 2. The extrapolation parameter S obtained from the plasma module. This figure shows only a part of the domain for clarity.

The chemistry module was a system of coupled ordinary differential equations, which were solved for the densities of 52 species, listed in table 4, and the 625 reactions associated with them. The

density of the i^{th} species in the chemistry module is given by equation 7. The full set of reactions can be found in [2] in addition to reactions obtained from [7,8] that are not included in [2].

$$\frac{\partial n_i}{\partial t} = R_i - \frac{n_i \mathbf{u}}{d} \quad (7)$$

In equation 7, n_i is the density of the i^{th} species, R_i is the rate expression of the i^{th} species, which is similar to that described in equation 3, \mathbf{u} is the velocity field at the point where the chemistry module is evaluated, which is calculated from the reactive flow module, and d is a characteristic length of the red coloured area shown in figure 2.

In table 4, the species are categorised based on their lifetimes into short-lived species, which are created and consumed every period, and long-lived species, which accumulate over multiple periods. This categorisation has been shown in many previous works [2,9].

Species type	Species list	Classification
Positively Charged	$N^+, N_2^+, N_3^+, N_4^+, O^+, O_2^+, O_4^+, H^+, H_2^+, H_3^+, OH^+, H_2O^+, H_3O^+, NO^+, N_2O^+, NO_2^+$	Short-lived
Negatively Charged	$e, O^-, O_2^-, O_3^-, O_4^-, NO^-, N_2O^-, NO_2^-, NO_3^-, H^-, OH^-$	Short-lived
Excited	$N(^2D), N_2(A^3\Sigma), N_2(B^3\Pi), O(^1D), O_2(a^1\Delta)$	Short-lived except $O_2(a^1\Delta)$ which is long-lived
Neutral	$H, N, O, NO, NO_2, NO_3, N_2O, N_2O_3, N_2O_4, N_2O_5, O_3, HNO, HNO_2, HNO_3, OH, H_2O_2, HO_2, H_2, N_2, O_2, H_2O$	Long-lived except H which is short-lived

Table 4. A list of species included in the chemistry module.

In addition to species densities, the chemistry module also solved for the electron temperature, according to equation 8.

$$\frac{\partial}{\partial t} \left(\frac{3}{2} n_e T_e \right) = P_{dep} - S_{en} \quad (8)$$

In equation 8, P_{dep} is the power deposition obtained from the plasma module at the center of the region of the area shown in red in figure 2, and S_{en} is the energy collisional loss computed by the chemistry module.

The chemistry module was solved for 10 periods of the assumed waveform, which was enough for the short-lived species to arrive at periodic behavior. In the last period, all the chemical reactions leading to generation of a long-lived species, N_2O as an example, from short-lived species were grouped together and averaged over the period's duration, giving an effective generation term g_{N_2O} , which represented the generation rate of N_2O from short-lived species. Similarly, the same procedure was followed for reaction where N_2O is consumed in reactions involving short-lived species, giving an effective loss term l_{N_2O} , which represented the loss rate of N_2O from reactions with short-lived species. Considering that loss reactions of N_2O include it as a reactant, the loss term l_{N_2O} was normalised by the density of N_2O . Two terms, g and l , were obtained for every long-lived species listed in table 4.

3. Reactive flow module:

The reactive flow module was a 2D time dependent multispecies module. Its computational domain included the plasma region and a downstream region, as indicated in figure 3. It was solved for the densities of the 21 long-lived species indicated in table 4 and their associated reactions (60 reactions), in addition to the velocity field of the mixture made of those species. The velocity field of the mixture was computed using Navier-Stokes equations 9-10 [10].

$$\frac{\partial \rho}{\partial t} + \nabla \cdot (\rho \mathbf{u}) = 0 \quad (9)$$

$$\rho \frac{\partial \mathbf{u}}{\partial t} + \rho \mathbf{u} \cdot \nabla \mathbf{u} = -\nabla P + \zeta \nabla^2 \mathbf{u} + \mathbf{F}_{EHD} \quad (10)$$

In equations 9 and 10, ρ is the mass density of the species mixture ($\text{kg}\cdot\text{m}^{-3}$), which was defined in terms of the individual species as $\rho = \sum_k m_k n_k$, such that m_k is the molecular mass (kg) of the k th species and n_k is its number density (m^{-3}), \vec{u} is the velocity field ($\text{m}\cdot\text{s}^{-1}$), ζ is the air's viscosity ($\text{Pa}\cdot\text{s}$), P is the pressure (Pa), and \vec{F}_{EHD} is the time-averaged EHD force field obtained from the plasma module. The time-averaged force field was used instead of the instantaneous force field given by equation 6 because the instantaneous force changed on a μs timescale, while the flow dynamics occurred on ms timescale. In that sense, the flow experienced the time-averaged force field rather than the instantaneous force field. To determine the densities of the reactive species, the convection diffusion equation was solved for 20 species, as given in equation 11 [11]. The remaining species, N_2 was determined from pressure constraint imposed by Navier-Stokes equations.

$$\frac{\partial n_i}{\partial t} + \nabla \cdot (-D_i \nabla n_i + n_i \vec{u}) = r_i + G_i - L_i n_i \quad (11)$$

In equation 11, n_i is the density of the i^{th} species (m^{-3}), D_i is the diffusion coefficient of the i^{th} species (m^2s^{-1}), obtained from [2], r_i is the rate expression of the i^{th} species ($\text{m}^{-3}\text{s}^{-1}$), which is similar to that in equation 3, except that it only involved reactions where species involved in the reaction were long-lived species only. The short-lived species were implicitly included in equation 11 through the terms G_i and L_i , which described the generation and loss rates of the i^{th} species due to short-lived species. These two parameters are defined by equation 12.

$$G_i = g_i S \quad (12)$$

In equation 12, g_i is the effective generation rate calculated by the chemistry module. Since it is a scalar and it needs to be converted to a 2D variable to be used by the reactive flow module, it was

multiplied by the extrapolation parameter S , shown in figure 2. The same procedure was followed to obtain L_i from l_i , as well.

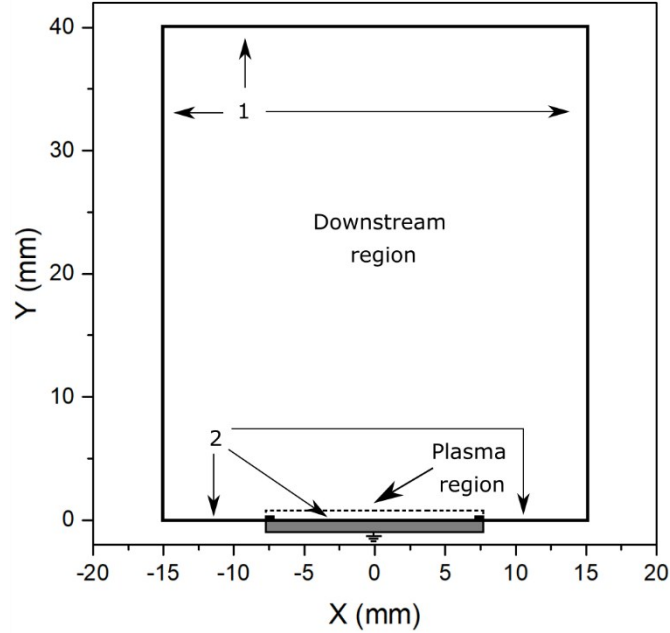


Figure 3. The computational domain of the reactive flow module. The plasma region is part of the computational domain. The electrodes are plotted as bold lines for illustration.

It should be noted that the time-averaged force field \vec{F}_{EHD} , the generation parameters G_i and the loss parameters L_i were all defined in the plasma region only (see figure 3), and were equal to zero elsewhere. For every equation solved in the reactive flow module, a boundary condition was defined over every edge in the computational domain. The boundary conditions are listed in table 5, where the number of the boundary is indicated in figure 3.

Boundary	Navier-Stokes equations	Convection diffusion equations
1	$\hat{n} \cdot \left[-PI + \zeta \left(\nabla \vec{u} + (\nabla \vec{u})^T \right) \right] = 0$	$-\hat{n} \cdot D_i \nabla n_i = 0$
2	$\vec{u} = 0$	$\hat{n} \cdot \left(-D_i \nabla n_i + n_i \vec{u} \right) = 0$

Table 5. The boundary conditions used in the reactive flow module.

In table 5, I is the identity matrix, and $(\nabla \mathbf{u})^T$ is the transpose of the gradient of the velocity vector.

The boundary conditions on boundary 1 described an open boundary, which implies that the other side of the boundary was continuation of the domain. Boundary conditions on boundary 2 described a wall, where the flow velocity was zero due to friction and the flux of the reactive species was zero.

References

[1] Chen F, Introduction to plasma physics and controlled fusion, 2nd edition, Springer 1984. Ch 3.

[2] Sakiyama Y, Graves D B, Chang H-W, Shimizu T & Morfill G E *J. Phys. D. Appl. Phys.* **45** 425201 (2012).

[3] Chen F, Introduction to plasma physics and controlled fusion, 2nd edition, Springer 1984. Ch 5.

[4] Hagelaar G J M and Pitchford L C *Plasma Sources Sci. Technol.* **14** 722 (2005)

[5] MORGAN database, www.lxcat.net, retrieved on 20 December 2016

[6] Boeuf J P and Pitchford L C *J. Appl. Phys.* **97**, 103307 (2005).

[7] Shimizu T, Sakiyama Y, Graves D B, Zimmermann J L and Morfill G E *New J. Phys.* **14** 103028 (2012).

[8] Bansemer R, Schmidt-Bleker A, Rienen U and Weltmann K-D *Plasma Sources Sci. Technol.* **26** 065005 (2017)

[9] Hasan M I & Walsh J L *J. Appl. Phys.* **119**, (2016).

[10] Kee R J, Coltrin M E, and Glarborg P, Chemically reacting flow theory and practice, John Wiley and sons 2003. Ch 3.

[11] Bird R B, Stewart W E, and Lightfoot E N, Transport Phenomena, 2nd edition, John Wiley and sons 2002. Ch 19.